Stability Research on Aerodynamic Configuration Design and Trajectory Analysis for Low Altitude Subsonic Unmanned Air Vehicle

Amer Farhan Rafique
Ph.D. Candidate, School of Astronautics
Beijing University of Aeronautics and Astronautics, China
Email address: afrafique@yahoo.com

He LinShu
Professor, School of Astronautics
Beijing University of Aeronautics and Astronautic
37 XueYuan Road, Haidian District, 100083, Beijing, China
Email address: helinshu@sina.com

Keywords: Aerodynamic Coefficients, Aerodynamic Forces, Aerodynamic Moments, Computational Fluid Dynamics, Six Degree of Freedom Trajectory Wind Tunnel

Abstract

In this paper a conventional approach for design and analysis of subsonic air vehicle is used. First of all subsonic aerodynamic coefficients are calculated using Computational Fluid Dynamics (CFD) tools and then wind-tunnel model was developed that integrates vehicle components including control surfaces and initial data is validated as well as refined to enhance aerodynamic efficiency of control surfaces. Experimental data and limited computational fluid dynamics solutions were obtained over a Mach number range of 0.5 to 0.8. The experimental data show the component build-up effects and the aerodynamic characteristics of the fully integrated configurations, including control surface effectiveness. The aerodynamic performance of the fully integrated configurations is comparable to previously tested subsonic vehicle models. Mathematical model of the dynamic equations in 6-Degree of Freedom (DOF) is then simulated using MATLAB/SIMULINK to simulate trajectory of vehicle. Effect of altitude on range, Mach no and stability is also shown. The approach presented here is suitable enough for preliminary conceptual design. The trajectory evaluation method devised accurately predicted the performance for the air vehicle studied. Formulas for the aerodynamic coefficients for this model are constructed to include the effects of several different aspects contributing to the aerodynamic performance of the vehicle. Characteristic parameter values of the model are compared with those found in a different set of similar air vehicle simulations. We execute a set of example problems which solve the dynamic equations to find the aircraft trajectory given specified control inputs.

Introduction

The Conceptual Design of any Air Vehicle starts with calculation of static and dynamic Aerodynamic Coefficients using CFD tools. This initial aerodynamic data forms the basis of further analysis. Extensive wind tunnel tests are then conducted to validate this data. The purpose of aerodynamic configuration design is to satisfy the trajectory determined by design mission.

The Static and Dynamic stability coefficients found through CFD tool FASTRAN are validated through Wind Tunnel tests. The aerodynamic performance characteristics of the proposed design are examined here using experimental force and moment data and computational predictions. Mach number and Angle of Attack variations effects are evaluated using experimental data. The longitudinal and lateral-directional stability characteristics are also examined.

A definitive measurement of the low-speed flight characteristics of vehicle under study is required to augment the overall design database for this important class of vehicles. These wind tunnel tests provided measurements of moments and forces about all three axes, control effectiveness, flow field characteristics and the effects of configuration changes.

Initial stability coefficients are further used in the Six-Degree of Freedom (DOF) SIMULINK model to predict and analyze the trajectory of air vehicle. Roll, Pitch and Yaw angles were found during initial flight phase and then subsequent commands were generated to cope with initial instability. Pitch angle variations were critical before auto pilot took over so it was also analyzed. Total time of flight was calculated using this model and effect of altitude is predicted and analyzed. Mach number and range variations were also to be analyzed.

The basic set of equations of motion of air vehicle serve as the mathematical model of the flight and these will be utilized to do analytical work and numerical simulation. Hence these equations of motion are theoretical basis for the flight dynamics. In the establishment of mathematical model a variety of factors are taken into account, such as;

- Aerodynamic forces and moments acting on vehicle body.
- Wind (gust or turbulence) in atmosphere.
- Action of the control/guidance system, deflection of control surfaces.
- Inertia values of vehicle.

Equations of Motion

Following are the force equations of motion [1] in body-fixed axis system along x, y and z respectively;

$$m(\dot{U} - VR + WQ) = -mg \sin\Theta + F_{Ax} + F_{Tx} \quad (1)$$

$$m(\dot{V} + UR - WP) = mg \sin\Phi \cos\Theta + F_{Ay} + F_{Ty} \quad (2)$$

$$m(\dot{W} + UQ - VP) = mg \cos\Phi \sin\Theta + F_{Ay} + F_{Ty} \quad (3)$$

Following are the moment equations of motion in body-fixed axis system;

$$I_{XX}\dot{P} - I_{XZ}\dot{R} - I_{XZ}PQ + (I_{ZZ} - I_{YY})RQ = L_A + L_T \quad (4)$$

$$I_{YY}\dot{Q} + (I_{XX} - I_{ZZ})PR + I_{XZ}(P^2 - R^2) = M_A + M_T \quad (5)$$

$$I_{ZZ}\dot{R} - I_{XZ}\dot{P} + (I_{YY} - I_{XX})PQ + I_{XZ}QR = N_A + N_T \quad (6)$$

Aerodynamic Angles

In aircraft aerodynamics the direction of air-stream velocity V with respect to the aircraft body [2] is expressed by two angles;

- Angle of Attack (AOA, α): angle between longitudinal axis X_B and projection of air-stream velocity V on plane of symmetry X_BV.
- Sideslip Angle (Beta, β): angle between plane of symmetry and air-stream velocity V.

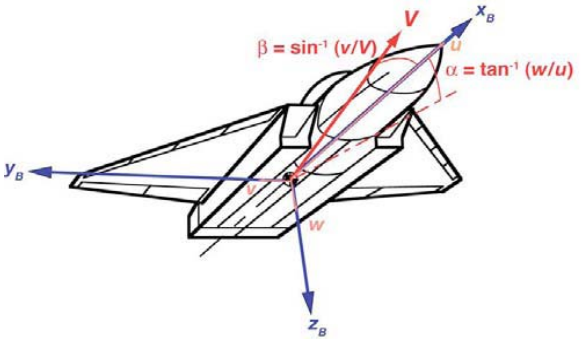

Fig 1: Aerodynamic Angles

Where;

$$\begin{bmatrix} u \\ v \\ w \end{bmatrix} = \begin{bmatrix} V\cos\alpha\cos\beta \\ V\sin\beta \\ V\sin\alpha\cos\beta \end{bmatrix} \quad (7)$$

And

$$\begin{bmatrix} V \\ \beta \\ \alpha \end{bmatrix} = \begin{bmatrix} \sqrt{u^2 + v^2 + w^2} \\ \sin^{-1}(v/V) \\ \tan^{-1}(w/u) \end{bmatrix} \quad (8)$$

Aerodynamic Forces

In aircraft aerodynamics there are three forces which occur during flight. These forces in body axis system [2] are as under;

- Lift Force (L): this is normal force perpendicular to x_b axis. Lift Force coefficient is C_L.
- Axial Drag Force (D): this is along x_b axis. Drag Force coefficient is C_D.
- Side Force (Y): this force is along y_b axis. Side Force Coefficient is C_Y.

Aerodynamic Moments

Aerodynamic moments in body axis or about centre of gravity (cg) are expressed in terms of moment coefficients [2], which are as follows;

Rolling Moment

$$M_x = (1/2)C_{mx}\rho V_a^2 S l \quad (9)$$

Pitching Moment

$$M_y = (1/2)C_{my}\rho V_a^2 S l \quad (10)$$

Yawing Moment

$$M_z = (1/2)C_{mz}\rho V_a^2 S l \quad (11)$$

These moments are generated by aileron deflection (δa, +ive for clockwise roll), (δe, +ive trailing edge down) and (δr, +ive trailing edge towards left and +ive for +ive sideslip) respectively.

Purpose of Study and Block Diagram

The purpose of the current study is to examine the aerodynamic characteristics of subsonic vehicles. The objectives of this study were twofold. The first was to create an experimental and computational database for feasible configurations. The second objective was to evaluate the controllability of fully integrated vehicle and the effectiveness of the control surface design. These objectives were accomplished using results from wind-tunnel testing and a limited number of computational fluid dynamics (CFD) solutions.

Block diagram of the approach followed is as under;

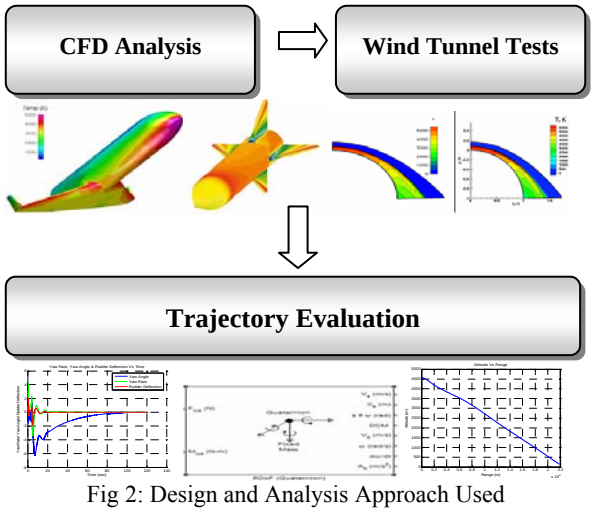

Fig 2: Design and Analysis Approach Used

Aerodynamic Analysis

CFD Analysis

A CFD technique based on Vortex Lattice Method (VLM) is used for treating the unsteady low speed aerodynamics of air vehicle. The main emphasis is placed on a practical, cost-effective engineering

solution of the complex problem with a reasonable computational efficiency allowing the computer code to run on small personal computers. VLM approach is one of the most efficient tools for complex geometries as it uses only a surface grid which is relatively easy to generate [3, 4].

Subsonic lift and drag data obtained CFD iterations are presented for different configurations for angles of attack and sideslip angles Mach numbers ranging from 0.5 to 0. 8. This data is further used in validation process from small-scale wind-tunnel tests.

Wind Tunnel Analysis (Static Stability Coefficients)

A series of wind tunnel test were conducted on the concept model of air vehicle to calculate the static stability coefficients. The Experiments were carried out in Transonic Wind Tunnel with a test section size of 760 x 530 mm. The tests were conducted on a 1/9th scale model of the air vehicle. The data obtained was utilized to obtain the complete set of static stability and performance data for use in the development of a final aero model.

Preliminary tests were conducted to determine tunnel flow offsets. In this regard model upright (0^0) and inverted (180^0) scans were conducted to determine α while model roll $+90^0$ and -90^0 tests were conducted to determine β offsets. In both the cases negligible offsets were measured. Initial tests were aimed at build-up analysis.

The tests were conducted in Mach range of 0.5 to 0.8. Elevator control power was tested using elevator angle of -2.5, -5 -7.5, -10 degrees. The rudder control power was measured by rudder deflection angles of +10 degrees where as aileron control power was measured by aileron deflection of +5 and +10 degrees.

Following equations were used to calculate Lift, Drag, Side force coefficients and Pitching, Yawing and Rolling moment coefficients respectively in body axis;

$$C_L = C_{Lo} + C_{L\alpha} \times \alpha + C_{L\delta e} \times \delta e \tag{12}$$

$$C_D = C_{Do} + KC_L^2 \tag{13}$$

$$C_Y = C_{Y\beta} \times \beta + C_{Y\delta r} \times \delta r \tag{14}$$

$$C_m = C_{mo} + C_{m\alpha} \times \alpha + C_{m\delta e} \times \delta e \tag{15}$$

$$C_n = C_{n\beta} \times \beta + C_{n\delta r} \times \delta r + C_{n\delta a} \times \delta a \tag{16}$$

$$C_l = C_{l\beta} \times \beta + C_{l\delta a} \times \delta a + C_{l\delta r} \times \delta r \tag{17}$$

Wind Tunnel Analysis (Dynamic Stability Coefficients)

Dynamic Stability tests were carried out with the purpose to measure dynamic stability co-efficient in the wind tunnel. These coefficients are required for the design of aerodynamics and control system of a flight vehicle. The tests were performed to reduce the uncertainty in damping derivative which are primarily C_{mq} (Pitching Moment), C_{nr} (Yawing Moment) and C_{lp} (Rolling Moment).

The dynamic derivatives were measured by means of free-oscillation method. In this technique the test model was installed on the balance through a flexural pivot for pitching tests and through a four beam flexures for rolling tests. A strain-gage-bridge stuck on the flexural beams to measure the output of voltage while the flexural beams were deflected. The sting mechanism comprised of automated variable pitch angle. Pure pitch or yaw angles were tested on the dynamic test rig.

The basic instrumentation system used for free-oscillation consists of the strain-gage-bridge, signal conditioner, oscilloscope, air-driven exciter and its controller, data acquisition system and a A/D converter, and a personal computer. The excitation system was pneumatic in nature. It consisted of a cylinder and piston linked with a push rod. At the other end of the push rod there was a pushing piece. The cylinder was mounted inside of the stiff support and high-pressure air from the air supply pushed the piston and then the push rod. The pushing piece moved forward or rearward, providing an angular displacement to the model.

The test was performed by generating a command from the computer which made the exciter push the model to have an initial angular displacement and then a release command is generated which causes the model to oscillate freely. The output of voltage from the strain-gage-bridge is conditioned and amplified by the signal conditioner. The time history of the angular displacement is recorded and converted into digital signals by the data acquisition system and the A/D converter and then saved in the computer. The data of the time history is then post-processed to calculate the damping derivatives. The test mechanism was intended to operate as a one-degree-of –freedom system in pitch, yaw or roll. The moment equation-of-motion of the test system, written in body axis, about the cross flexure pivot, while wind off [5], is

$$I\ddot{\theta} - M_{\dot{\theta}_0}\dot{\theta} - M_{\theta_0}\theta = 0 \tag{18}$$

Where I is the moment of inertia, $M_{\dot{\theta}_0}$ is the mechanical damping moment, M_{θ_0} is the cross flexure stiffness.

The solution of Eq. (13) is

$$\theta = \theta_{\max} e^{-M_{\dot{\theta}_0}\omega_0^2 t/2M_{\theta_0}} \cos\left[\omega_0\sqrt{1-\left(\frac{M_{\dot{\theta}_0}\omega_0}{2M_{\theta_0}}\right)^2}\,t\right] \tag{19}$$

Since

$$\left|\frac{M_{\dot{\theta}_0}\omega_0}{2M_{\theta_0}}\right| << 1 \tag{20}$$

It follows that, approximately,

$$\theta = \theta_{\max} e^{-M_{\dot{\theta}_0}\omega_0^2 t/2M_{\theta_0}} \cos\ \omega_0 t \tag{21}$$

Where

$$\omega_0^2 = -\frac{M_\theta}{I} \tag{22}$$

$$\omega_0 = 2\pi f_0 \tag{23}$$

Where, f_0 is the natural frequency of model-balance system.

Eq. (21) is exactly a curve of a damping period function and its sequence peaks are as follows:

$$\theta_p = \theta_{\max} e^{-N\pi M_{\dot{\theta}_0}\omega_0 / M_{\theta_0}} \quad (24)$$

From Eq. (24), it follows that

$$M_{\dot{\theta}_0} = \frac{M_{\theta_0} \ln\left(\frac{\theta_i}{\theta_0}\right)}{\pi\omega_0 (N_i - N_0)} \quad (25)$$

Where θ_0 and θ_i are the amplitude corresponding to peak N_0 and N_i respectively.

From the bench test, the frequency f_0 and sequence θ_i and N_i are measured. And by using of least square method we could have

$$K = \frac{\ln\left(\frac{\theta_i}{\theta_0}\right)}{N_i - N_0} \quad (26)$$

And then

$$M_{\dot{\theta}_0} - \frac{M_{\theta_0} K}{\pi\omega_0} \quad (27)$$

Similarly, for wind tunnel tests the equation of motion of the model-balance system is;

$$I\ddot{\theta} - (M_{\dot{\theta}} + M_{\dot{\theta}_0})\dot{\theta} - (M_{\theta} + M_{\theta_0})\theta = M_0 \quad (28)$$

And the sequence of the peak of the damping period curve is;

$$\theta_p = \theta_{\max} e^{-N\pi (M_{\dot{\theta}} + M_{\dot{\theta}_0})\omega_0 / M_{\theta_0}\omega} \quad (29)$$

where ω is the round frequency of the model-balance system. We could also have ;

$$M_{\dot{\theta}} = -\frac{M_{\theta_0}\omega K}{\pi\omega_0^2} - M_{\dot{\theta}_0} \quad (30)$$

6-DOF Simulink Model

We describe the equations of motion developed for fixed mass zero-thrust (gliding) aircraft model operating in an environment of spatially varying atmospheric winds. The wind/ gust effects are included as an integral part of the flight dynamics equations, and the model is controlled through the three aerodynamic control angles. Formulas for the aerodynamic coefficients for this model are constructed to include the effects of several different aspects contributing to the aerodynamic performance of the vehicle. 6-DOF Quaternion solver is used which integrates the 6 degree of freedom equations of motion using a quaternion representation for the orientation of the body in space. The integration of the rate of change of the quaternion vector is given below. The gain K drives the norm of the quaternion state vector to 1.0 should □ become nonzero. The value of this gain is very critical and to be chosen with care, because a large value improves the decay rate of the error in the norm, but also slows the simulation because fast dynamics are introduced. An error in the magnitude in one element of the quaternion vector is spread equally among all the elements, potentially increasing the error in the state vector.

$$\begin{bmatrix}\dot{q}_0\\ \dot{q}_1\\ \dot{q}_2\\ \dot{q}_3\end{bmatrix} = 1/2\begin{bmatrix} q_3 & -q_2 & q_1\\ q_2 & q_3 & -q_0\\ -q_1 & q_0 & q_3\\ -q_0 & -q_1 & -q_2\end{bmatrix}\begin{bmatrix}p\\ q\\ r\end{bmatrix} + K\varepsilon\begin{bmatrix}q_0\\ q_1\\ q_2\\ q_3\end{bmatrix} \quad (31)$$

Where;

$$\varepsilon = 1 - \left(q_0^2 + q_1^2 + q_3^2 + q_4^2\right) \quad (32)$$

The Quaternion selection conforms to the previously described equations of motion. Initial position in inertial axes [Xe Ye Ze], Initial velocity in body axes [U v w], Initial Euler rotation [roll pitch yaw] in radians, Initial body rotation rates [p q r] in radians per second, Initial mass of the rigid body, A 3-by-3 inertia matrix for the full inertia of the body. Inertia matrix which is used in 6-DOF solver is given as [6];

$$(I)_b = \begin{pmatrix} I_{xx} & -I_{xy} & -I_{xz}\\ -I_{xy} & I_{yy} & -I_{yz}\\ -I_{xz} & -I_{yz} & I_{zz}\end{pmatrix} \quad (33)$$

The Wind Shear Model [7, 8] block adds wind shear to the aerospace model. This implementation is based on the mathematical representation in the Military Specification MIL-F-8785C. The magnitude of the wind shear is given by the following equation for the mean wind profile as a function of altitude and the measured wind speed at 20 feet (6 m) above the ground.

$$u_w = W_{20}\frac{\ln(h/z_0)}{\ln(20/z_0)}, \quad 3\text{ft} < h < 1000\text{ft} \quad (34)$$

Where u_w is the mean wind speed, W_{20} is the measured wind speed at an altitude of 20 feet, h is the altitude, and z_0 is a constant. The resultant mean wind speed in the Earth-fixed axis frame is changed to body-fixed axis coordinates by multiplying by the direction cosine matrix (DCM) input to the block. The block output is the mean wind speed in the body-fixed axis.

Results

Wind Tunnel

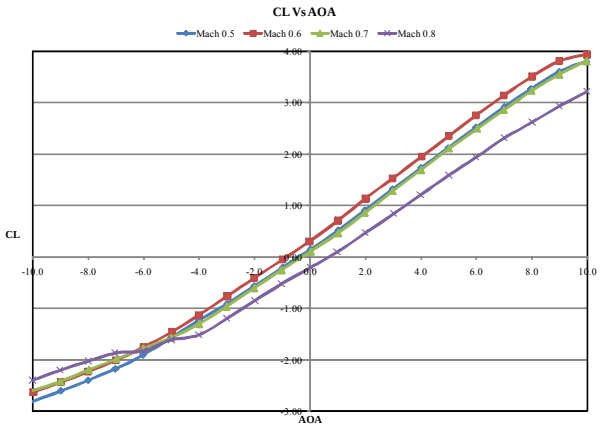

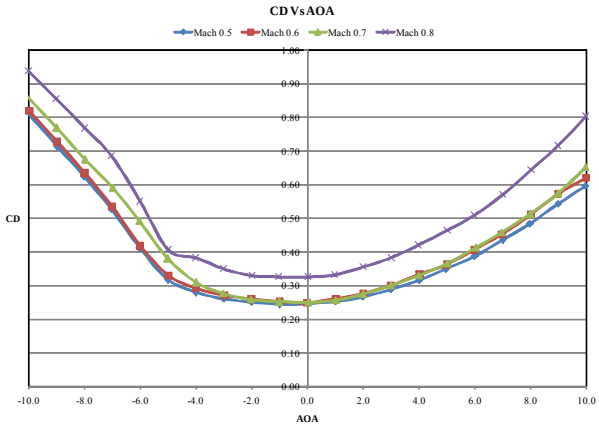

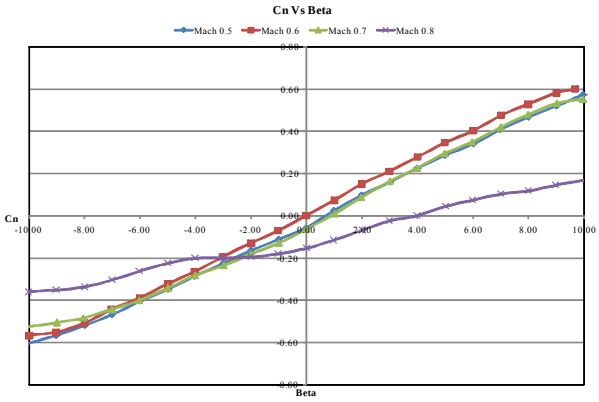

Fig 4: Moment at Mach 0.5, 0.6, 0.7, 0.8

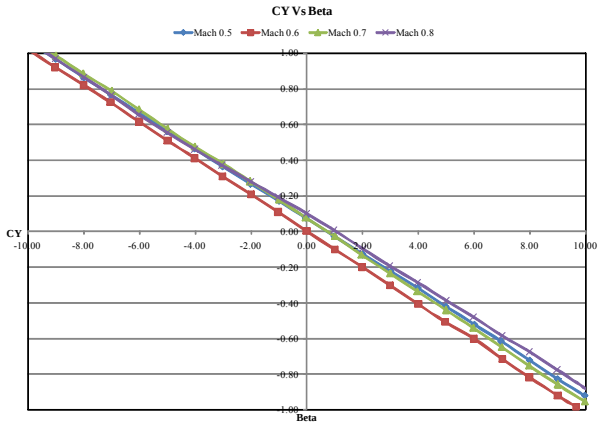

Fig 3: Lift, Drag and Side Force at Mach 0.5, 0.6, 0.7, 0.8

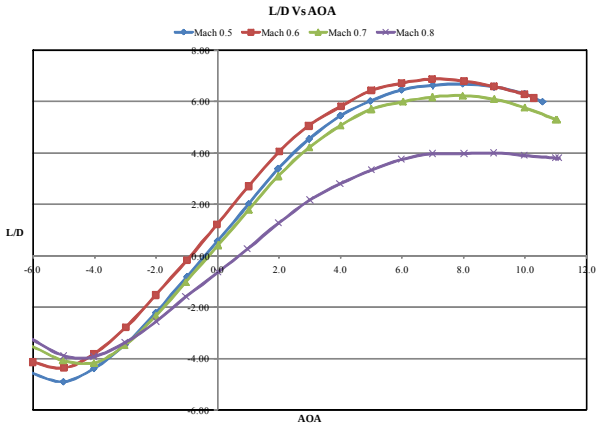

Fig 5: L/D Vs AOA at Mach 0.5, 0.6, 0.7, 0.8

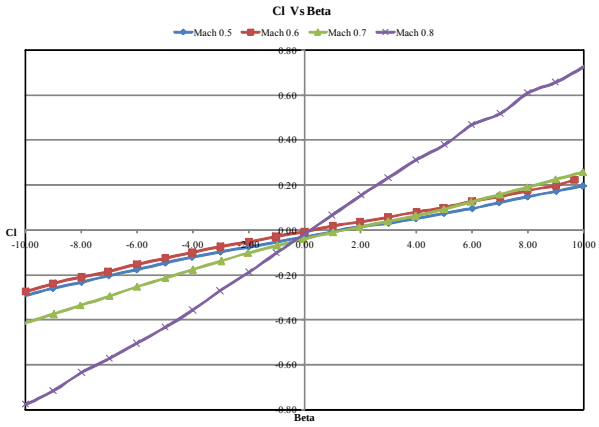

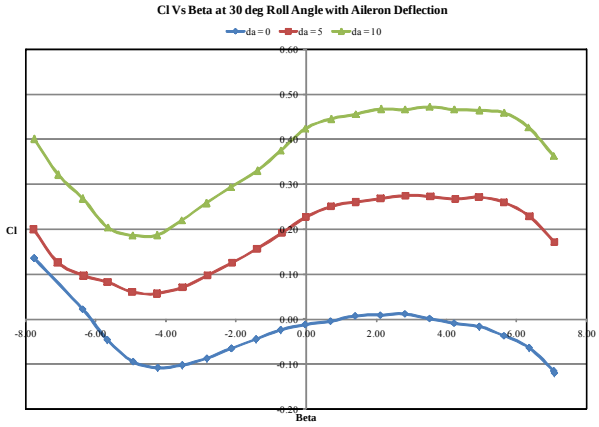

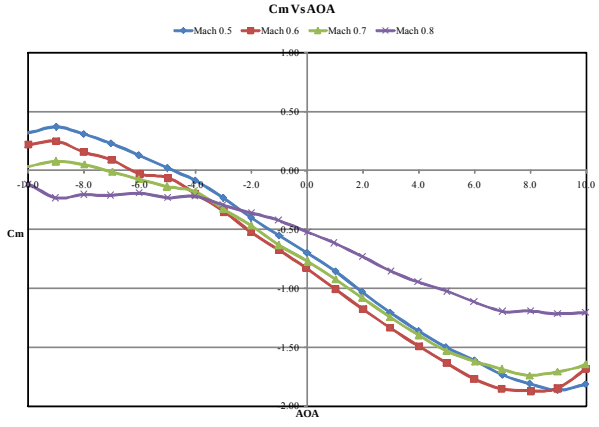

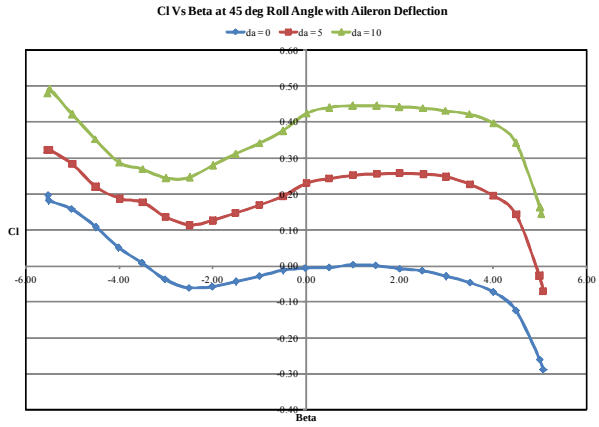

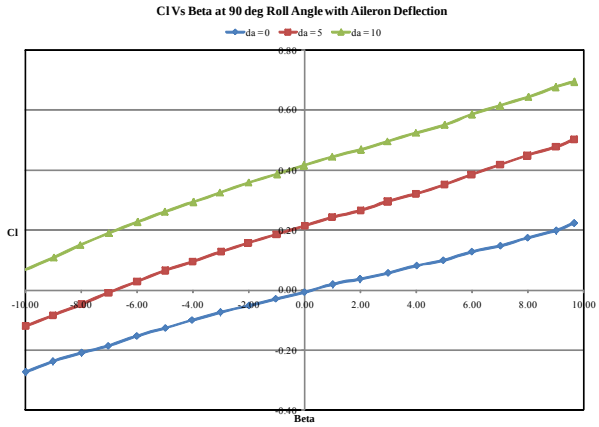

Fig 6: C_l Vs Beta with δa at Roll Angles of 30^0, 45^0, 90^0

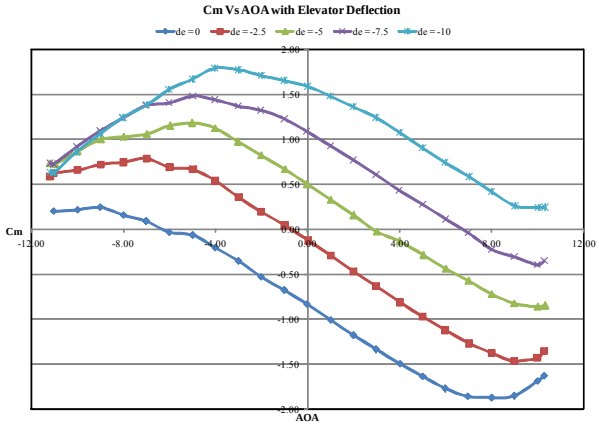

Fig 7: Cm vs AOA with δe

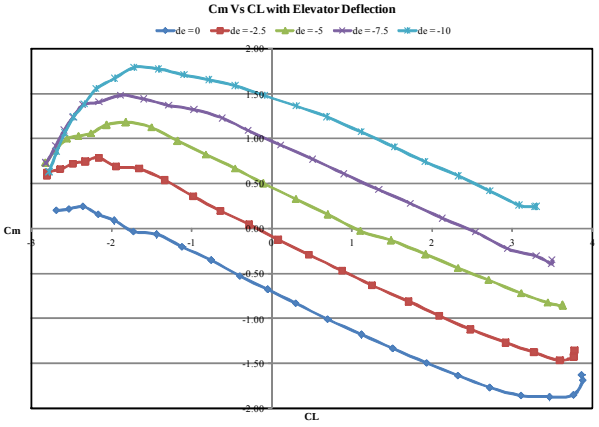

Fig 8: C_mC_L vs AOA with δe

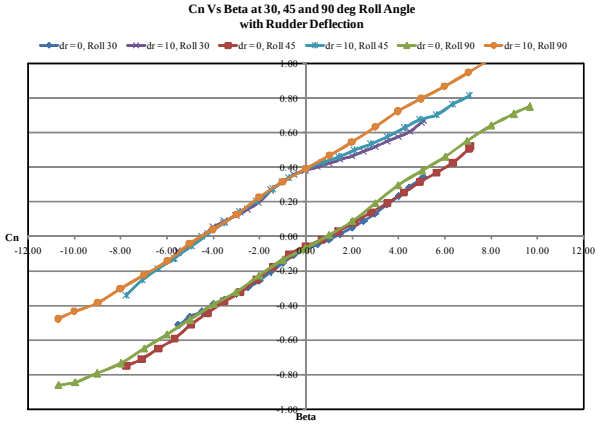

Fig 9: C_n Vs Beta with δr at Roll Angles of 30^0, 45^0, 90^0

Trajectory

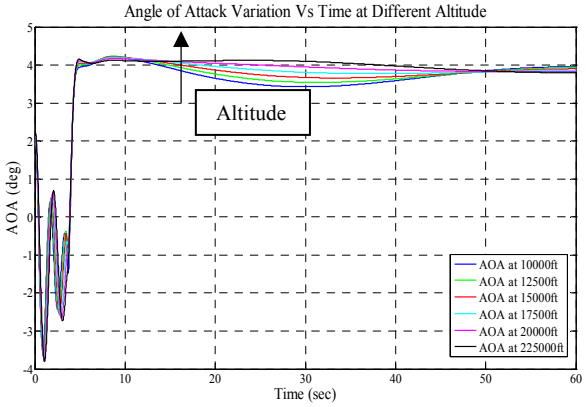

Fig 10: AOA Variation with Time wrt Altitude

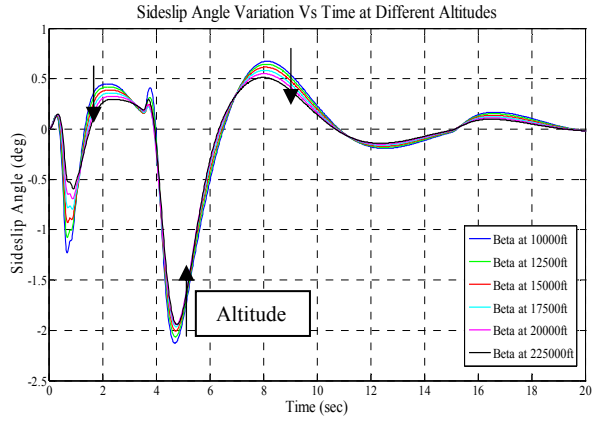

Fig 11: Beta Variation with Time wrt Altitude

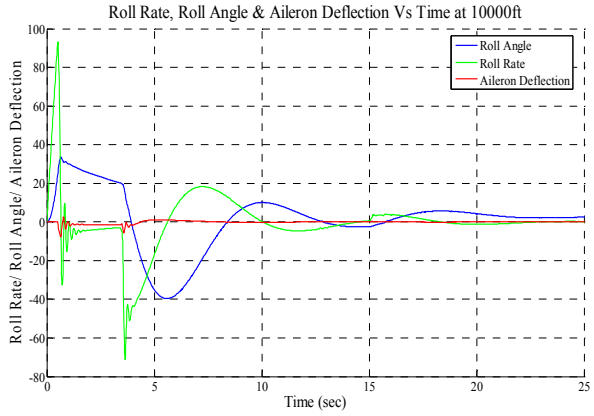

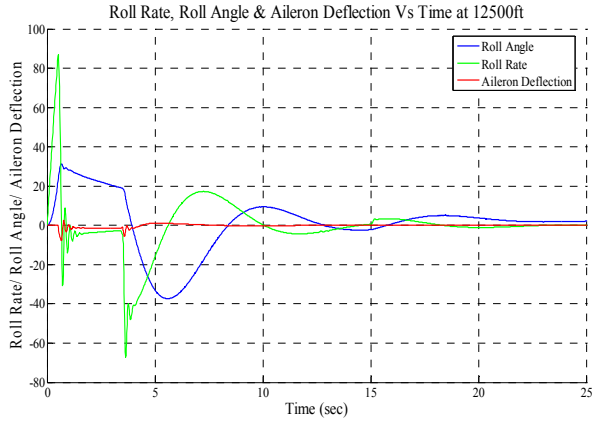

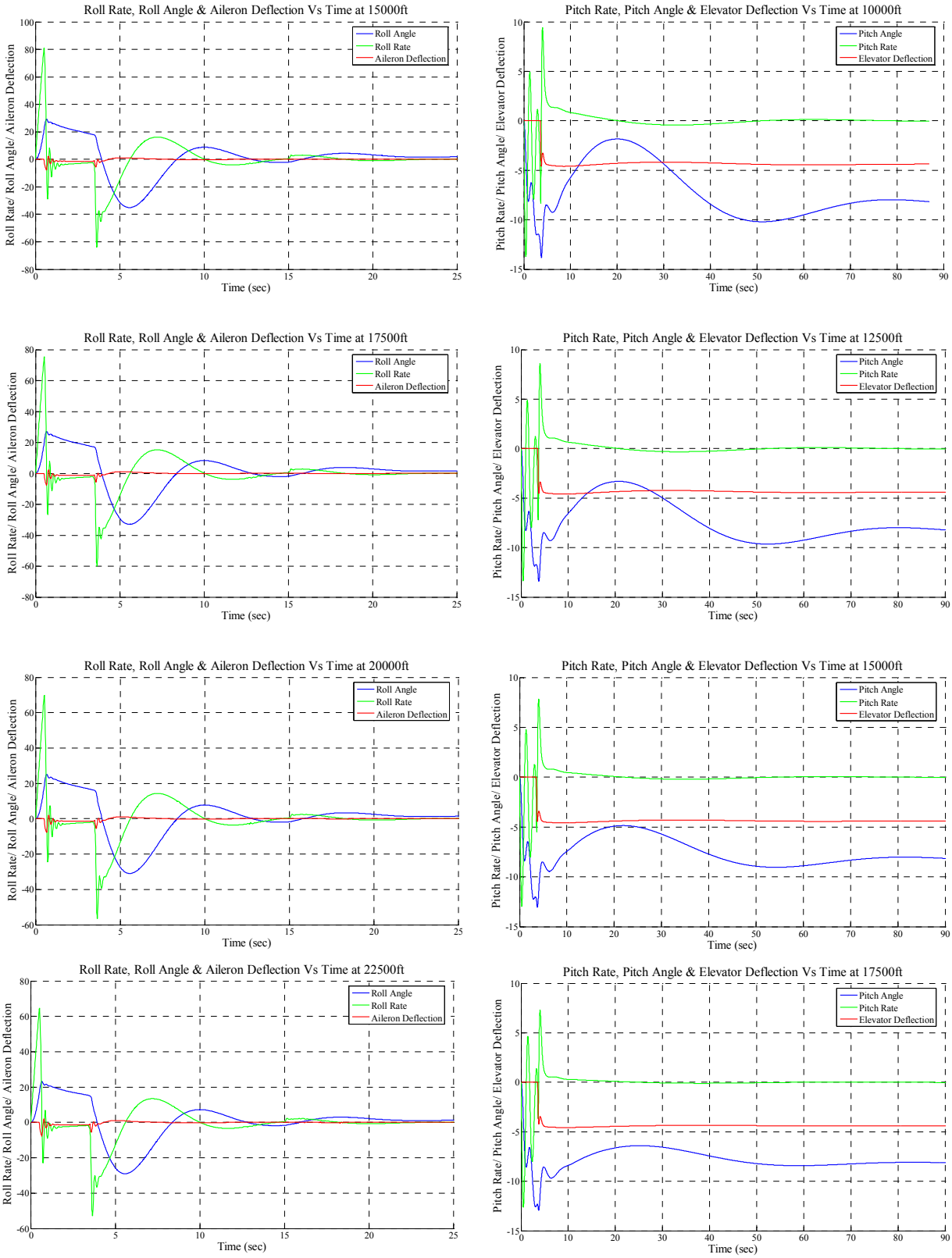

Fig 12: Roll Rate, Roll Angle and δa wrt Altitude

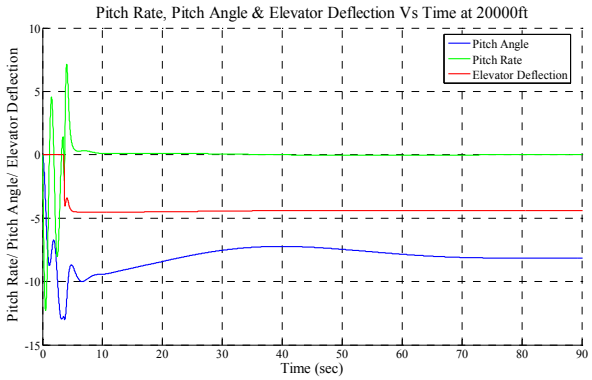

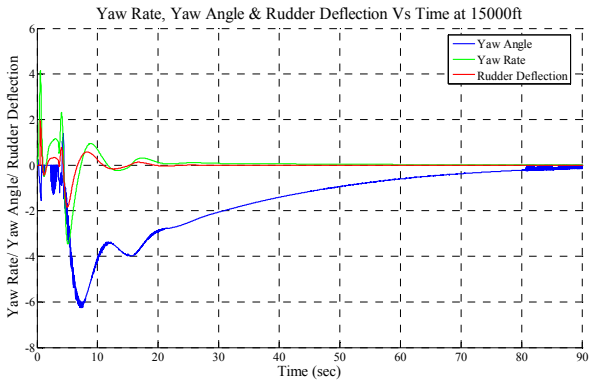

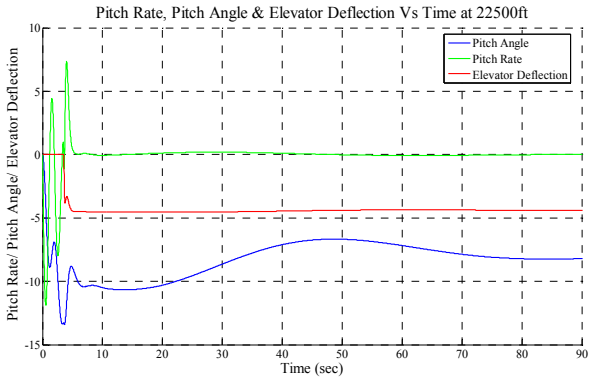

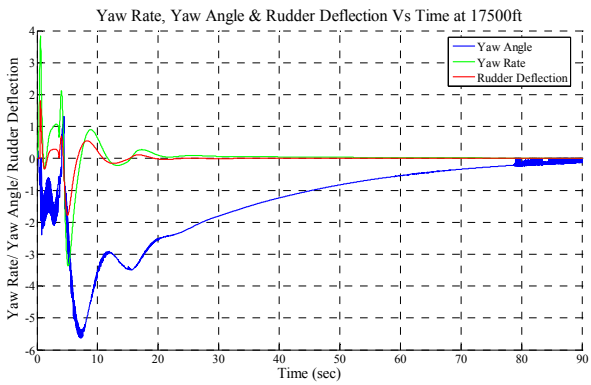

Fig 13: Pitch Rate, Pitch Angle and δe wrt Altitude

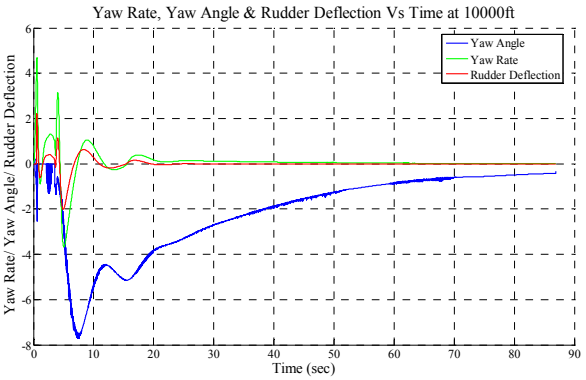

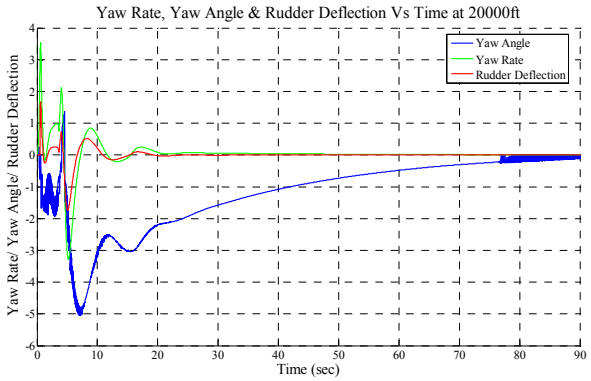

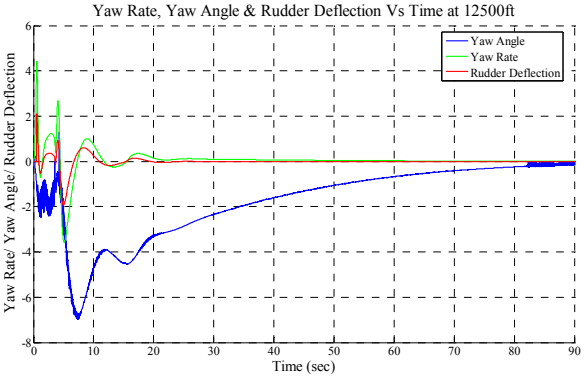

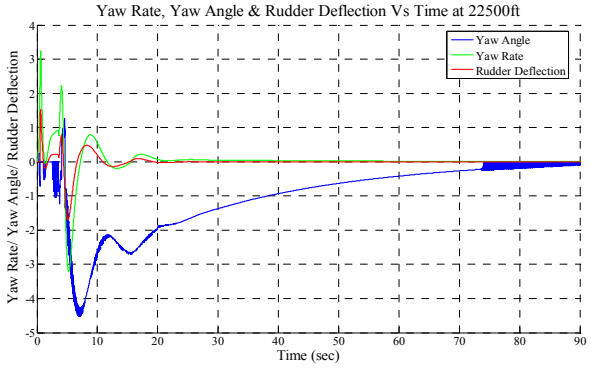

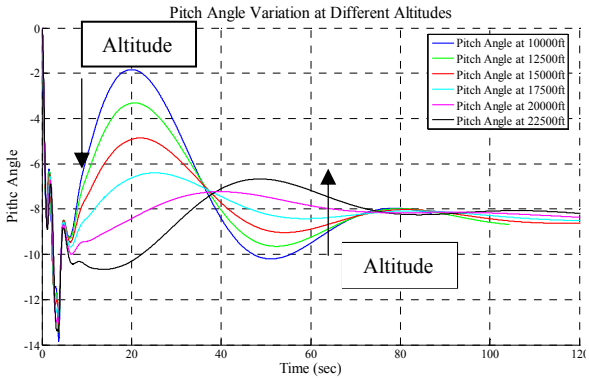

Fig 14: Pitch Angle Variation wrt Altitude

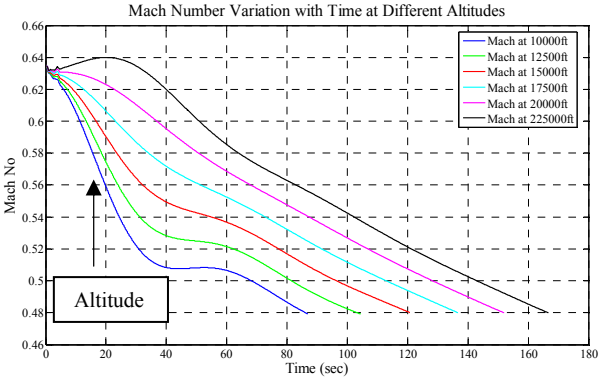

Fig 15: Mach No Variation with Time wrt Altitude

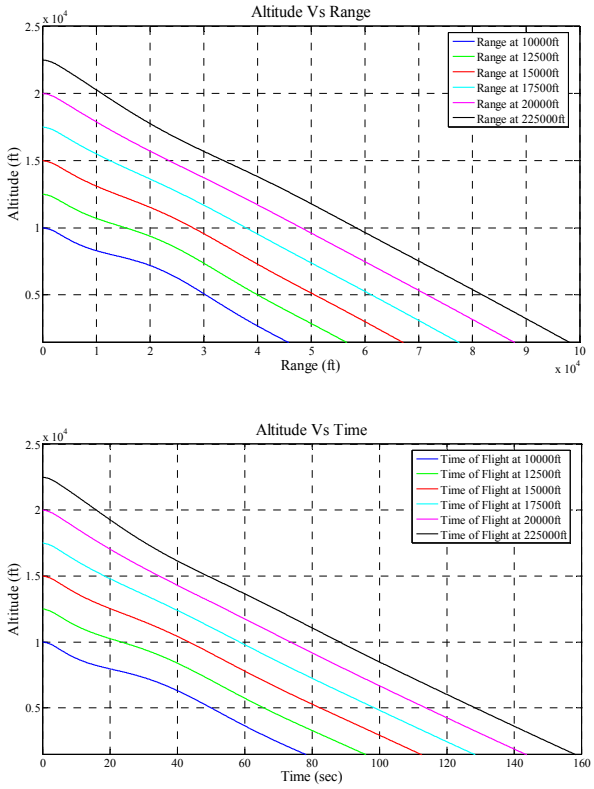

Fig 16: Time of Flight

Discussion of Results

- The yaw stability is a function of aileron deflection angle. The air vehicle would show a yawing affect if one of the tail stalls. This happens once local angle of attack on any surface would exceed 7 degrees. The results indicate that for $|\alpha| + |\delta a| < 7.5$ the yawing moment co-efficient does show cross coupling with angle of attack, but it does not become unstable. The actual cross-coupling can be measured by pure beta sweeps at different angles of attack.
- The air vehicle is neutrally stable in roll. This implies that it would have very low rolling tendency with side-slip angle.
- The roll control power remains constant for $|\alpha| + |\delta a| < 8$ degrees. Once this limit exceeds the roll control power starts to decrease.
- The air vehicle stalls at 10 degree angle of attack.
- L/D vs AOA is plotted and found that $\alpha_{L/Dmax}$ is 6 degree.
- Yaw stability slightly increases with angle of attack.
- Rudder control power is not a function of angle of attack.
- The air vehicle is neutrally stable in roll. This implies that it would have very low rolling tendency with side-slip angle.
- The aileron and rudder efficiency remains almost constant till 7 degree AOA but slightly decreases after 9 degree of AOA.
- Natural aerodynamic response of complete vehicle during initial flight phase when autopilot is inactive comes to be stable.
- During initial flight phase roll rate increased sharply which may cause structural failure.
- Pitch angles will have effect on lateral loads and thus limiting structural design.
- The perturbations caused by variation in altitude effects performance of vehicle.
- Propulsion system is excluded from this analysis to check aerodynamic stability of vehicle. In future work propulsion system will be incorporated and detailed analysis will be performed.

Conclusion

This analysis validated the wind tunnel data through trajectory simulation. Aerodynamic stability and control effectiveness of vehicle is also checked. This analysis can form base line for design of servo actuator system of control surfaces and can be used in controller design.

The proposed analysis approach is good enough for preliminary conceptual design and can be used for any type of air vehicles like waveriders, gliders, missiles, rockets, aircraft and unmanned aerial vehicles.

Stability research done in this study will form the baseline for bringing improvements in future. Stability data obtained will be used to improve the aerodynamics of vehicle under study.

References

1) Jan Roskam: Airplane Flight Dynamics and Automatic Flight Controls, Part 1, 1995.
2) Xiao YeLun: Rocket Ballistics and Dynamics, Beijing University of Aeronautics and Astronautics, 2005.
3) Konstadinopoulos, P., Thrasher, D.F., Mook, D.T.,Nayfeh, A.H. and Watson, L.: A Vortex-Lattice Method for General, Unsteady Aerodynamics, Journal of Aircraft, 22, No. 1, 1985, pp.43-49.
4) Rusak, Z., Seginer, A. and Wasserstorm, E., Convergence Characteristics of a Vortex-Lattice Method for Nonlinear Configuration Aerodynamics, Journal of Aircraft, Vol. 22, No. 9, 1985.
5) G. K. Batchelor, An Introduction to Fluid Dynamics, Cambridge University Press, Cambridge, England, 1967.
6) He Lin Shu: Launch Vehicle Design, Beijing University of Aeronautics & Astronautics, Beijing, China, 2005.
7) Sobieczky, H., Geissler, W.: Active Flow Control Based on Transonic Design Concepts, DLR German Aerospace Research Establishment, AIAA 99-3127,1999.
8) H. Schlichting, "Boundary-Layer Theory", McGraw-Hill, New York, 1979.

Appendix A

Nomenclature

α	AOA, Angle of Attack in Degrees
β	Beta, Angle of Sideslip in Degrees
δa	Aileron Deflection
δe	Elevator Deflection
δr	Rudder Deflection
c	Mean Wing chord
cg	Centre of Gravity
q	Free-Stream Dynamic Pressure
C_D	Drag Coefficient
C_L	Lift Coefficient
C_y	Side Force Coefficient
C_m	Pitching Moment Coefficient
C_l	Rolling Moment
C_n	Yawing Moment Coefficient
C_{mq}	Dynamic Pitching Moment Coefficient
C_{nr}	Dynamic Yawing Moment Coefficient
C_{lp}	Dynamic Rolling Moment Coefficient
S_{ref}	Reference Area